

## Inference of fault and fracture systems beneath the Matatlan waste dump basement, a VLF study

Miguel Ángel Alatorre-Zamora\*, José Oscar Campos-Enríquez, Salvador Isidro Belmonte-Jiménez and Jaime Ibarra-Nuño

Received: December 13, 2012; accepted: November 20, 2013; published on line: July 01, 2014

### Resumen

Se utilizó la técnica VLF para inferir zonas de fallas o de grandes fracturas que pudiesen servir como conductos para fluidos de desechos contaminantes en el vertedero de Matatlán, en Guadalajara, al oeste de México. Para interpretar los datos se usaron los filtros de Fraser y de Karous-Hjelt.

Se interpretaron perfiles de forma directa empleando el filtro modificado de Karous-Hjelt. Se aplicaron los filtros de Fraser y de Karous-Hjelt conjugados a todos los datos. Los resultados de ambas técnicas muestran similitud en las posiciones y orientaciones de rasgos anómalos que se asocian a zonas de fracturas o de fallas. Se observa una zona de falla en el centro del sitio, que tiene un rumbo NEE-SWW. Otros rasgos importantes inferidos tienen direcciones NW-SE y se observan en la parte occidental del área.

El uso conjunto de las técnicas basadas en los filtros de K-H y de Fraser dan resultados como una estructura N-S inferida en el límite occidental del vertedero, así como rasgos anómalos de dirección NW-SE, principalmente en la mitad occidental del

sitio. La estructura N-S tiene la misma dirección que el Cañón del Río Grande de Santiago, mientras que los rasgos NW-SE coinciden con las direcciones del rift Tepic-Zacoalco. Hacia el centro del área aparecen otros rasgos con direcciones NE-SW. Todos estos rasgos y sus direcciones coinciden de manera fuerte con la predominancia de grupos de fracturas mostrados en el análisis estadístico de fracturas, y podrían servir como conductos para la migración de lixiviados hacia el Cañón Coyula, al sur, y hacia el Cañón del Río Grande de Santiago, al este del sitio.

Un análisis estadístico de direcciones de fracturas mostró 4 direcciones principales N-S (A), N75-80E (B), N60-65W (C) y N25-30W (D), y dos direcciones secundarias que son N45-55E (E) y 90E (F). El patrón primario A coincide con la dirección del Cañón del Río Grande de Santiago, mientras que el patrón secundario F tiene una dirección paralela a la del Cañón Coyula.

Palabras clave: very Low Frequency, vertedero de Matatlán, zonas de fracturas, distribución de corriente, filtros Fraser y Karous-Hjelt.

---

M.A. Alatorre-Zamora\*  
Departamento de Ingeniería Civil y Topografía  
Centro Universitario de Ciencias Exactas e Ingeniería  
Universidad de Guadalajara  
\*Corresponding author: [alatorre2004@hotmail.com](mailto:alatorre2004@hotmail.com)

J.O. Campos-Enríquez  
Instituto de Geofísica  
Universidad Nacional Autónoma de México  
Delegación Coyoacán, 04510  
México D.F., México

S. Belmonte-Jiménez  
Centro Interdisciplinario de Investigación  
para el Desarrollo Integral Regional  
Instituto Politécnico Nacional  
Unidad Oaxaca

J. Ibarra-Nuño  
Departamento de Física  
Universidad de Guadalajara

## Abstract

We used the VLF technique to infer fault or major fracture zones that might serve as path for contaminant waste fluids in the Matatlan dumpsite, in Guadalajara, western Mexico. To interpret the data we used the Fraser, and Karous-Hjelt filters.

Profiles were interpreted with 2D direct modeling based on Karous-Hjelt modified filter (K-H). The Fraser and Karous-Hjelt conjugated filter were applied to the entire data. The results of both techniques show similarities in the directions and positions of anomalous features, which are assumed fault or fracture zones. We observed one fault zone at the centre of the site, with a NEE-SWW strike. Other important inferred structures have NW-SE directions at the western part of the site.

The cooperative use of both techniques, based on K-H filter and the Fraser filter give results as an N-S inferred structure in the westernmost part of the zone, as well as NW-SE linear anomalies, mainly in the

western half of the site. The N-S structure has the same direction as that of Rio Grande de Santiago Canyon. The NW-SE features coincide with the directions of the Tepic-Zacoalco rift. Others NE-SW lineaments are located towards the centre of the area. These facts coincide strongly with the predominance of fracture groups show in the fracture analysis. The inferred structures could serve as conduits for the leachates to migrate towards the Coyula canyon as well as towards the Rio Grande de Santiago Canyon.

Statistic analysis of fracture orientations showed N-S (A), N75-80E (B), N60-65W (C), and N25-30W (D) main directions, and N45-55E (E), and 90E (F) secondary directions. Group A coincides with the direction of the Rio Grande de Santiago Canyon, whereas pattern F have the same direction as Coyula Canyon.

Key words: Very low frequency, Matatlan dumpsite, fracture zones, current distribution, Fraser and Karous-Hjelt filters.

## Introduction

Very Low Frequency technique (VLF) is based on measurements of parameters of the polarization ellipse arising from the vector sum of magnetic components of primary and secondary electromagnetic fields. Primary VLF field sources are generated by powerful transmitting antennas specially designed for transoceanic communication; these antennas are disseminated in the north hemisphere. Several antennas do not transmit actually, representing a disadvantage for the method. The frequency of some transmitters have changed over time; for example, Cutler, Maine (NAA), transmitting with 17.8 kHz in 1970 (after Paterson and Ronka, 1970), transmitted in 1996 with 24.8 kHz, and Jim Creek, Washington (NLK/NPG) transmitting with 18.6 kHz, now transmits with 24.0 kHz. The VLF band itself has been modified: 15-25 kHz (Kaikkonen, 1979), 10-30 kHz (Olsson, 1980), and 15-30 kHz (Beamish, 1994).

The emitted primary field travels along the entire world, and at distances of more than 100 km, its magnetic component is almost horizontal and perpendicular to the source azimuth (Bozzo *et al.*, 1994). In presence of a conductor, the primary EM field penetrates into the ground and generates a secondary field that interacts with the primary field. The resultant field is controlled by the electric structure of

ground. This field is elliptically polarized and characteristics of magnetic secondary field can be represented by polarization ellipse parameters. In particular, two parameters of this ellipse are usually used to analyze the secondary field: the tilt angle  $\alpha$  (inclination of major axis) and the eccentricity or ellipticity  $e=H_z/H_x$  (the rate between minor and major axis). Moreover, since secondary field intensity is always smaller than primary field intensity, they can be written as

$$\alpha = Re/Hp \quad e = Im/Hp$$

(see for example, Saydam, 1981; Sinha, 1990a) and therefore it is possible to evaluate both in-phase,  $Re$ , and out-phase or quadrature,  $Im$ , components, both normalized with respect to the  $H_p$  main field.

Considering main components of the polarization ellipse, tilt angle and ellipticity would be:

$$\tan 2\alpha = \frac{2(H_z / H_x) \cos \Delta\phi}{1 - (H_z / H_x)^2}$$

and

$$e = \frac{H_z H_x \sin \Delta\phi}{H_1^2}$$

Where  $\phi$  is a tilted angle (it is a wavelit parameter).

Tilt angle tangent and ellipticity are good approximations to in-phase and quadrature components of vertical secondary field, respectively; both components can be employed to represent those components in acceptable limits, and to conduit an interpretation of results.

### Applications

VLF method is widely used in detection and delineation of shallow conductors as well as in groundwater exploration and in engineering studies. The method has been combined with seismic and magnetic methods to locate and to investigate fractures and cavities in carstic environments, which constitutes an engineering and hydrogeology problem (Armadillo *et al.*, 1998); also has been used in mineral location (Bayrak, 2002), in Earth surface structure studies (Alexandros *et al.*, 1999), in filtration studies of oil derived products at groundwater (Benson, *et al.*, 1997), in archaeological zones, or in monitoring and assessing impact from volcanic areas, in geological mapping, and particularly to locate narrow fault zones (Phillips and Richards, 1975). In particular, VLF has been employed with success in sites with pollution problems (Greenhouse and Harris, 1983), and in studies from mineralized areas (Paál, 1968; Paterson and Ronka, 1971).

One of the main impacts produced by dumpsites is ground and surface water contamination, caused by leachates. The contamination may lasts over 20 or 30 years after closure of the dumpsite (Kjeldsen *et al.*, 2002; Jones and Dixon, 2005; Christensen *et al.*, 2000; Bekaert *et al.*, 2002). A leachate is the liquid that seeps to lower levels of ground and extracts, dissolves or suspends materials. The VLF method is very sensitive to water quality, as well as to the presence of hydrocarbons. Pollution is often favored by the presence of large fractures and faults that acts as conduits for the migration of contaminating fluids. The VLF method is also sensitive to the presence of wet faults and fractures.

In this work is described a study in which the VLF method was applied with success to infer fractures. The case comprises an urban waste dumpsite, located at western Mexico. VLF data in this area are analyzed with Fraser (1969) and Karous-Hjelt (1983) techniques. At the dumpsite, it is expected to recognize ground areas contaminated with leachates. Fracture measurements

support the presence of the path-sources inferred by mean of VLF anomalies.

### Study area description

The area corresponds to the urban waste Matatlan dumpsite of Guadalajara, Jalisco, at western Mexico (Figure 1a). This dumpsite is named Matatlan that has been developed on top of a small plateau at the edge of the Rio Grande de Santiago Canyon; this Canyon limits to the north and east, the Guadalajara urban area (Figure 1b). It comprises andesitic flows intercalated with rhyolitic emissions from Cerro de la Reyna (Figure 1b). This dumpsite started to work in 1989, receiving about 800 tons per day, and closed in 2004 with a daily uptake of 1,500 tons.

A private company controlled the dumpsite several years, interspersed the waste with soil and coarse grain geologic material, constituted mainly by andesitic and tobaceous fragments; in this way, organic matter degradates and non-contaminant organic gases are expelled to the atmosphere.

During summer there exists a large quantity of leachates, when rainy season occurs. Although there are catchment pits for the leachates in the edges of the site, high grade fracturing at the andesitic basement could permit without-control migration of leachates outside the dumpsite; this could impact in a severe way the Canyon environment, considered as a natural area that should be environmentally protected.

### Adjacent local geology

The dumping site is located in an island-plateau, surrounded by three canyons. Coyula Canyon surrounds the site at its southwestern limits, along the southern, and almost all its western portion to turn then into an E-W direction to join the N-S to NW-SE Rio Grande de Santiago Canyon. In the north, the study area is limited by a small canyon that also intersects the Rio Grande de Santiago Canyon with an E-W to NE-SW direction (Figure 1b).

Dumpsite geologic features correspond to a boundary environment between two major geologic provinces: the Sierra Madre Occidental (SMOc) and the Trans-Mexican Volcanic Belt (TMVB) (Figure 1a). Both provinces impose their structural signature at the dumpsite. The dumpsite basement is formed by basaltic andesites and acid tuffs, according to petrographic analysis (Alatorre-Zamora, 2003). These volcanic products seem to proceed from

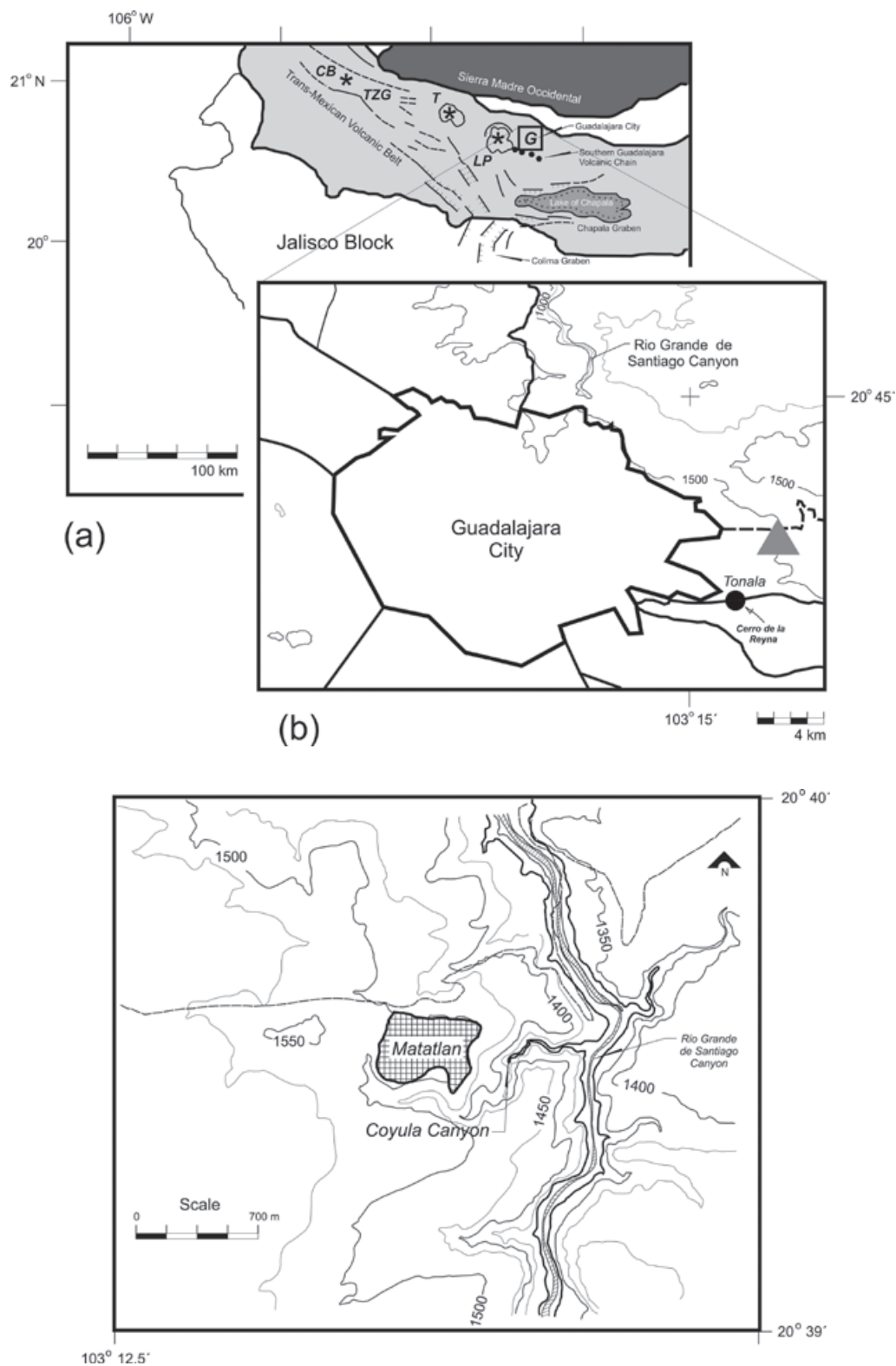


**Figure 1.** (a) Western Mexico showing main geologic features. CB-Ceboruco volcano; TZG- Tepic-Zacoalco Graben; T-Tequila volcano; LP-La Primavera Caldera; G-Guadalajara urban area. (b) Detail of Guadalajara City and Matatlan dumping site location, marked with a gray triangle at the east of Guadalajara. A black circle south of the grey triangle indicates the position of the andesitic volcano Cerro de la Reyna. The topographic curves are in meters above sea level. (c) Detailed topography at Matatlan dumping site; the Rio Grande de Santiago Canyon is clearly observed.

Cerro de la Reyna volcano. The outcroppings exhibit a high fracture degree (Figure 2) due to a combination of tectonism (characterizing a secondary porosity) with fractures originated at cooling lava moment (characterizing a primary porosity). Tectonic origin is proposed by observation of fault striae in the outcrops, although fractures due to listric movements are also possible.

First geological works in neighboring areas were done by Watkins *et al.* (1971), Mahood (1980), Gilbert *et al.* (1985) and Luhr and Lazaar (1985). The surrounding area is characterized by volcanic rocks successions, mainly pumitic deposits with ignimbrites, rhyolites, andesites and basaltic andesites intercalations. Into this general volcanic sequence the San Gaspar and Guadalajara ignimbrites are distinguished as good stratigraphic indicators (Gilbert *et al.*, 1985); standing out also are the so-called Guadalajara and San Cristobal groups, both from the Río Grande de Santiago Canyon and the Los Altos plateau, respectively.

The zone is surrounded by major faults. Neotectonic control from Quaternary volcanic activity reveals NW-SE alignments one of which is approximately tangent to Guadalajara urban area (Luhr and Lazaar, 1985; Alatorre-Zamora and Campos-Enríquez, 1991; Rosas-Elguera and Urrutia-Fucugauchi, 1998). Extensions occurring from Late Miocene at the Guadalajara area have been postulated in response to an initial opening of the S of California Gulf (Ferrari, 1995).

## Methodology

### Equipment

Equipment used in this case-study is an OMNI MAG Scintrex VLF equipment with three channels (Wright, 1988), to have access to three transmitting stations. For its management one must know both the locations and frequency of power stations and parameters as provided by the instrument itself.

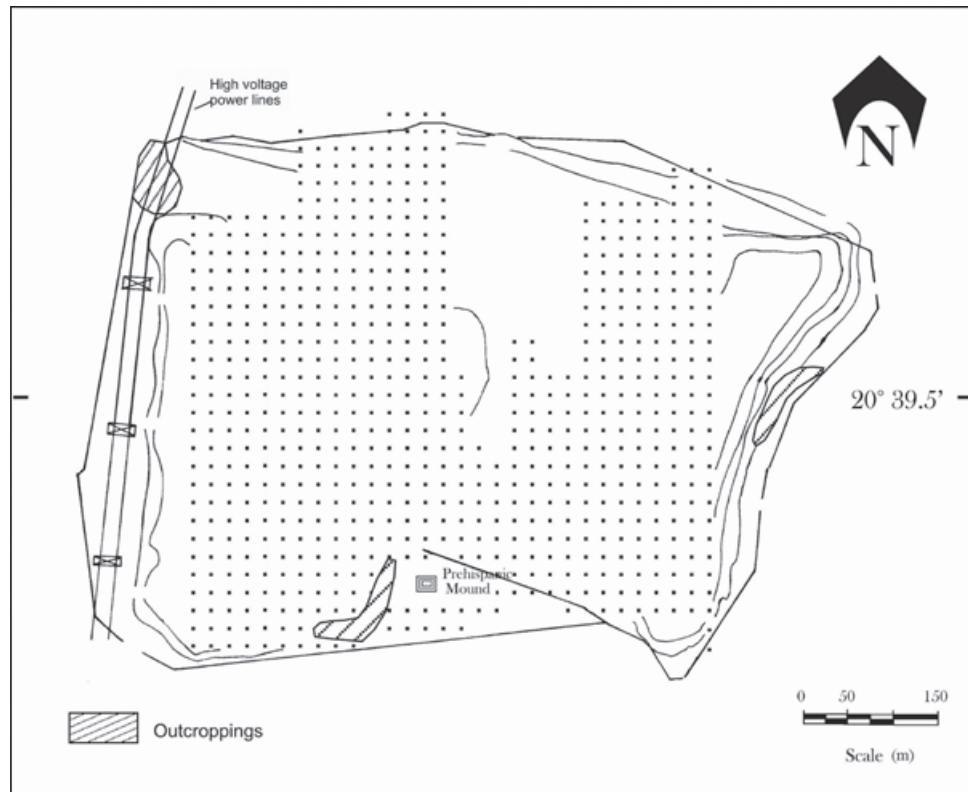


**Figure 2.** Detailed diagram of the Matatlan dumpsite. Points are measuring stations, with 20 m of separation. The box in the south is a pre-Columbian mound, whereas the boxes with two lines in diagonal, along the west side, correspond to towers of high-voltage wire lines. Andesitic outcrops, showed as shaded areas, are indicated. The continuous lines that surround the site are indicators of the limits and topography.



The OMNI MAG measures in-phase ( $H_x$ ) and quadrature (imaginary,  $H_y$ ) components normalized with the main field, along with complementary information as primary field intensity and tilt angle. In VLF methods both electric and magnetic components can be used. However, currently only the magnetic field  $H$  is used, because it is easier to calculate. In fact, the vertical component  $H_z$  is analyzed, as it is generated only by induction phenomena. The main field  $H_p$  lies almost in the horizontal plane.

#### VLF data

In Matatlan dumpsite, measurements were realized in 1997 along N-S profiles. NAA (located in Cuttler, Maine), NLK/NPG (located in Jim Creek, Washington State) and NPM (located in Lualualei, Hawaii) stations were used, with respective frequencies of 24.8, 24.0 and 23.4 kHz (see Table 1). At the time of these measurements NAA station showed a weak signal-to-noise ratio, so we decided to work with NLK/NPG station signal, assuming the presence of perpendicular structures to line of sight of this station. These measurements were taken each 20m, forming the data grid shown in Figure 2. In some areas it was not possible to conduct measurements because of dumping works were been conducted at that time. High-voltage N-S transmission lines are located at the western side of the dumpsite (Figure 2). A lineal distance near to 80 meters separates the measurement area from high-voltage lines.

#### VLF anomalies processing

Traditionally, the interpretation of VLF tilt angle data was conducted qualitatively. VLF quantitative interpretation owes its beginnings to Fraser (1969) and Karous and Hjelt (1983) filtering techniques. However, as with other geophysical methods, VLF first interpretation techniques are based on the use of simple

geometric bodies (Paterson and Ronka, 1978). Baker and Myers (1979) from laboratory modeling obtain VLF responses similar to that obtained by Paterson and Ronka (1978), who employ analytic methods.

A realistic VLF modeling of the subsurface must take into account media with different conductivities, irregular geometry and anisotropy to model VLF anomalies (Kaikkonen, 1979). So far, these factors are difficult to incorporate in numerical models to account for real geologic situations. Models from Vozoff (1971), Ward *et al.* (1974) and Kaikkonen (1979) are applicable to very simple structural situations and do not include the effect from conductive shields (covers). The high electric conductivity of these shields avoid the EM wave transmit to depth; this behavior reduces the searched thickness and produces a marginal penetration beneath the surface. Thickness and electric conductivity of the upper layer (or uppermost cover) control the VLF response (Olsson, 1980).

In a direct interpretative process Kaikkonen (1979) employs a finite element formulation starting from Maxwell equations in the frequency domain, to model ellipticity, tilt angle and amplitude ratio; he uses isotropic and anisotropic models of an inclined dike encased in a resistive media. With the ellipticity and the tilt angle it is possible to discriminate between good and poor conductors. Both parameters have same polarity for a poor conductor, but ellipticity changes polarity and shape for a good conductor (Kaikkonen, 1979).

One of the first VLF inversion methods was developed by Olsson (1980), that approaches an integral equation as a system of equations which is solved by iterative numerical techniques (Olsson, 1980). In this way, response curves for different models with a conductive cover are obtained. Since

**Table 1.** VLF stations used in Matatlan dumpsite.

Station	Operative Frequency for 1997	Operative Frequency for 2007	Location
NAA	24.8 KHz	17.8 KHz	Cuttler, maine (40° NE of Matatlan)
NLK/NPG	24.0 KHz	18.6 KHz	Jim Creek, Washington (20° NW of Matatlan)
NPM	23.4 KHz	23.4 KHz	Lualualei, Hawai (90° W of Matatlán)

then, several inversion methods have been developed, including 1-D inversion (Hjelt *et al.*, 1985), regularized bidimensional inversion (Beamish, 1994), 3-D inversion (Beamish, 1998), and VLF and VLF-R data joint inversion using simulated annealing (Kaikkonen and Sharma, 1998). In one case Hjelt *et al.* (1985) work with VLF-resistive data, which is an extension from conventional VLF-Z (Beamish, 1994) or VLF-EM techniques (Reynolds, 1998). In VLF-R information from just one frequency is obtained, measuring perpendicular components of electric and magnetic horizontal fields, giving in this manner impedance values. Beamish (1994) and Kaikkonen and Sharma (1998) also work with VLF-R data. Beamish (1994) makes an extension from a non-linear inversion techniques for MT data to VLF-R measurements, employing a 2-D Occam procedure.

In this study we applied the filtering techniques of Fraser and Karous-Hjelt, as primary approximations to an interpretation of VLF data.

#### *Fraser filter*

Fraser filtering comprises a process applied to data profiles whose results can be contoured. This method (Fraser, 1969) is designed for those parameters that exhibit a response with zero crossings, as in the in-phase vertical component ( $H_z$ ) or the tilt angle of the polarization ellipse ( $\alpha$ ). In this method horizontal gradients are calculated and parts of the data are smoothed, so as to place the maximum value over a conductive surface. This is obtained with the following relation (Bayrak, 2002),

$$F_{2,3} = (M_3 + M_4) - (M_1 + M_2) \quad (1.1)$$

where F are the stations, the subscript are the station numbers, whereas  $M_1$  to  $M_4$  are consecutive tilt angle stations (Bayrak, 2002). This anomaly is antisymmetric over conductors, and is often indicated as gradient. The anomaly is convolved along several profiles, with the filter adjusting its length to the anomaly shape.

The interpretation of the results is qualitative. Very sharp responses indicate shallow sources, whereas wide anomalies progressively indicate deeper sources.

#### *Karous-Hjelt filter*

A very interesting technique for interpreting VLF data is based on the filter designed by Karous and Hjelt (1983), that although is a

direct modeling technique, provides good locations of bodies and underground features giving rise to VLF anomalies. Karous and Hjelt (1983) based its algorithm on Biot-Savart law to describe the surface magnetic field of a 2-D distribution. They assume a small horizontal layer, with several current densities located at a depth equal to the distance between stations. When this method is used for data correction, results can be contoured as a proxy of conductivity as a depth function.

The idea of modeling VLF-EM data by mean of Karous-Hjelt filtering technique consists basically in considering subsurface electric heterogeneities as giving rise to current lines that distort primary EM fields. The developed lineal filter is applied in conjunction with a lowpass filter. As result this method provides a vertical distribution of apparent current densities (López-Sánchez, 1998). These current densities are associated with conductive zones below the surface (Marroquin, 2000).

Formulation of Karous-Hjelt filter for calculating current density,  $I(0,)$  is

$$I(0) = k (-0.102H_{-3} + 0.059H_{-2} - 0.561H_{-1} + 0.059H_2 + 0.102H_3) \quad (1.1)$$

where  $k$  depends from station interval and  $H_n$  is the  $n$ -th stations behind (-) or forward (+) of filtered station (0).

We have employed academic computer programs developed by Edsen and Nissen (1997) and Pirttijärvi (2004); the first one forms the direct models with cells with constant resistivities and variable dimensions and depths. The second one applies both the Fraser, and Karous-Hjelt filters. The interpretation of the profiles obtained in this study was done in two steps.

## **Results and discussions**

### *Fracture measurements*

A Brunton compass was used to measure orientation of a wide group of fractures along the three existing outcroppings located inside and around the dumpsite limits (Figure 2).

The southern and northern outcrops consist of densely fractured basaltic andesites, whereas that to east comprises andesites plus altered tuffs (Figure 2).

The orientation of the fractures were plotted in a polar histogram with divisions each five degrees (Figure 3). The statistic analysis shows

the presence of primary and secondary fracture groups. Among the primary groups the most conspicuous has a North-South direction; the second one has N75-80E orientation; the third one has a mean azimuth of N60-65W direction, and the last one has a N25-30W direction. There are two secondary alignment groups that may be related to the primary directions. The most clear of them presents a N45-55E orientation, whereas the last one is outlined with a 90E direction. These fracture groups are referred to as A to F, respectively (Figure 3). Pattern A coincides with the direction of the Rio Grande de Santiago Canyon, whereas pattern F has the same direction as Coyula Canyon in its main part.

#### VLF parameters

Although the kind of information provided by the VLF method must be filtered to be represented in contour maps (what emphasizes positive features), it was decided to first present in raw form the in-phase, the out-of-phase, and tilt angle. Using triangular interpolation, we contoured the respective maps of the VLF parameters showed at Figures 4a, 4b, and 5a. These results will now be qualitatively interpreted.

Frequently occurring fluctuations in VLF measurements are not caused by temporal

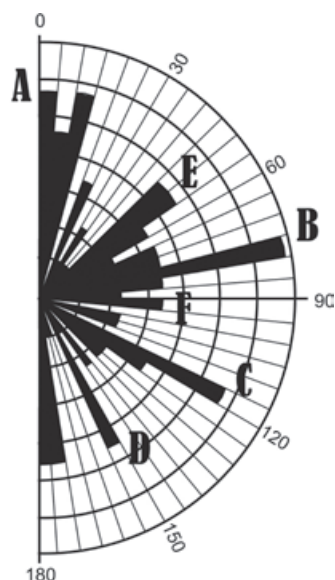


**Figure 3.** Polar histogram from fracture pattern measurements in andesitic outcrops showed in the Figure 2. The divisions are given each 5°. The letters indicate main directions of groups of fractures.

or spatial variations of the signal. These variations are attributed to anthropogenic noise and often have a typical morphology. Along the western boundary runs a high voltage line but its noisy effect (high amplitude and strong separation between components after Bozzo *et al.*, 1994) is not as obvious as the effect induced by the metallic fence that surrounds a pre-Columbian mound, at the south center of the area (Figures 4a, 4b and 5a). The effect of the high voltage lines can be observed only in the first 40 m approximately, whereas the wire fence surrounding the pre-Columbian mound produces an effect due to its high conductivity. Its influence is still observed at approximately 70 meters away from the mound (see Figures 4a, 4b and 5a).

Conspicuous anomalies in the in-phase and the out-of-phase components, (Figures 4a and 4b) occur at points where leachate ponding is very extensive (A in Figures 4a to 5b). An interesting observation that arises from the comparison of the two maps is the north-south elongated feature of the central part, which is positive in both components (B in Figures 4a and 4b) but is accompanied by a negative in the in-phase component (referred to C in Figures 4a and 5a). In addition, areas of deposition and new mixed garbage at the date of the VLF survey are clearly visible as closed anomalies (D in Figures 4a to 5b). This behavior prevails in the northeastern part of the landfill, which is seen as a major negative pattern in the in-phase component (Figure 4a).

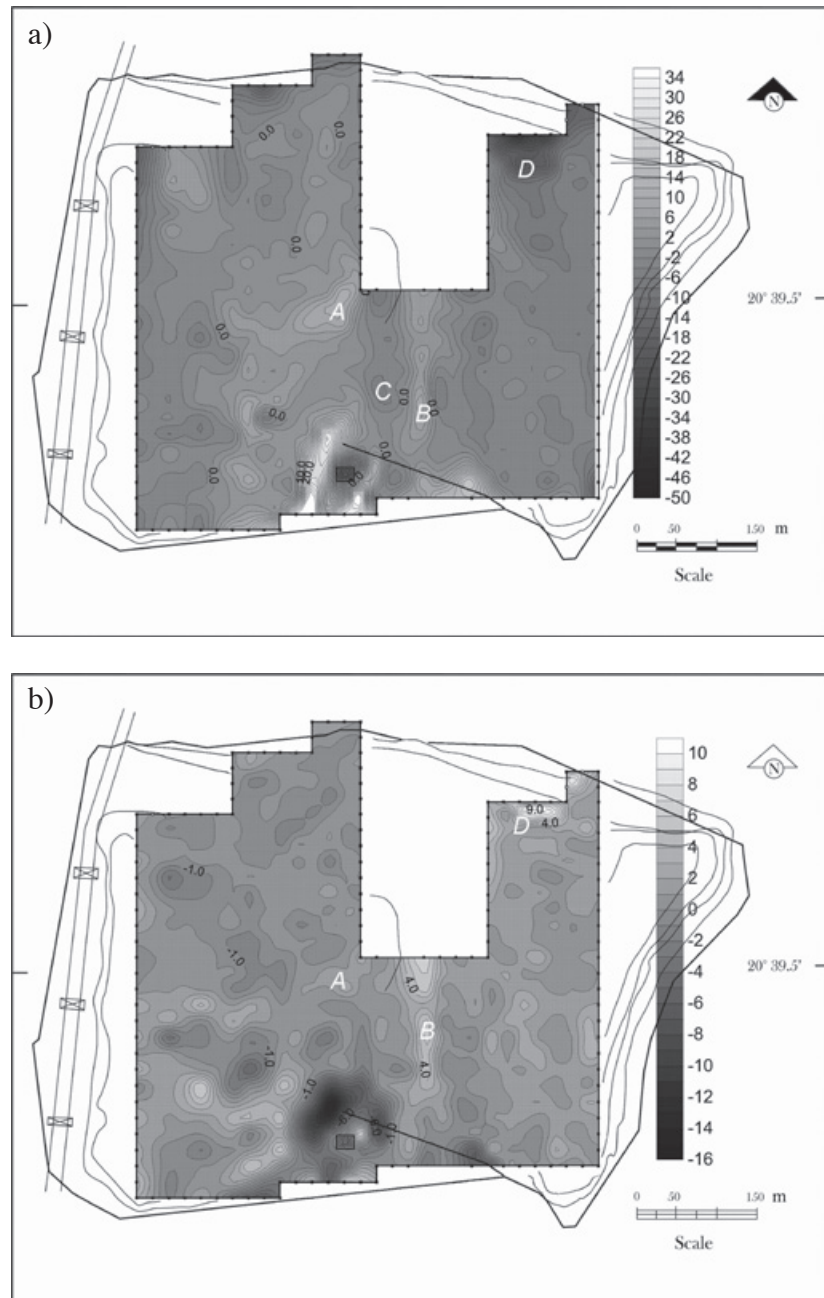
Many times the VLF response simply can not be interpreted. This is due to overlapping effects of other anomalies, and attenuation and phase change induced by conductive cover.

Certainly, the bulk of the interpretation in the VLF method remains up today qualitative in nature. In fact, until 1980 the interpretation was mainly based on qualitative arguments, neglecting the influence of rock covers and guest conductors (e.g., Olsson, 1980). A more complete interpretation should include the recognition of type anomaly selecting a general model type, and some rudimentary analysis to locate depths to the source. In addition, some general idea would be obtained about, for example, the conductivity of the target.

The differences between tilt angle (Figure 5a) and its respective 3D Fraser-filtered map (Figure 5b) are more or less significant. One of these differences is that the elongated N-S minimum located at centre of the dump in the tilt angle map (C in Figure 5a) has



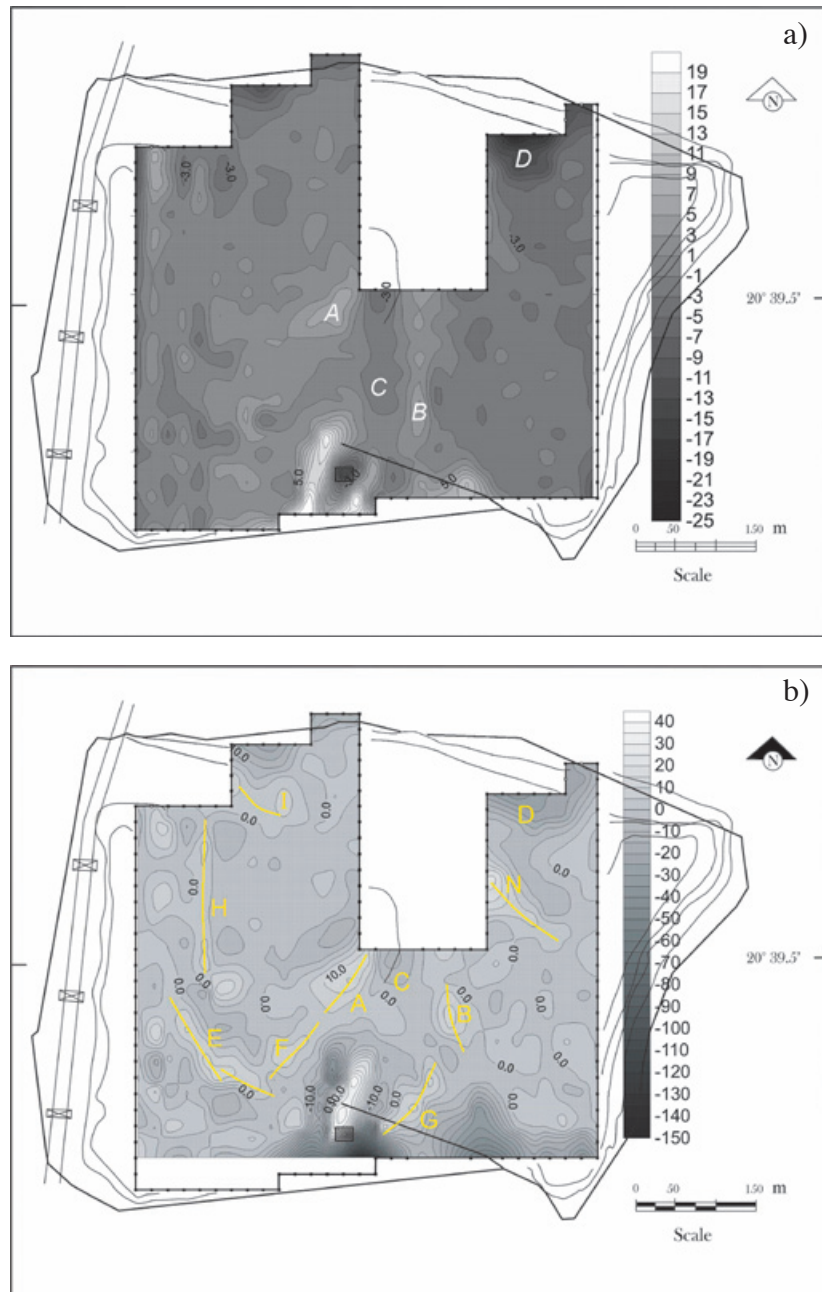
**Figure 4.** (a) VLF field in-phase component contoured each 2.0 %. Values in the scale at the left side are in %. The letters indicate most conspicuous anomalous features. (b) VLF out-of-phase component contoured each 1%. Values in the scale at the left side are in %. The letters indicate most conspicuous anomalous features.



been smoothed and eastward displaced in the filtered map (Figure 5b). Main positive features in the filtered map could be interpreted in two ways: 1) the elongated positive feature on the west side (E in Figure 5b) may be due to a structure roughly oriented NW-SE that acts as conduit for leachate, and 2) the positive feature referred to as A in Figure 5b, might be due to an accumulation of lixivates. Altogether, three main groups of elongated anomalies can be noted. In the western half and in the

centre occurs the major quantity of elongated positive anomalies, with NW-SE, N-S, and NE-SW orientations (A, E, F, H, and I in Figure 5b), whereas in the eastern portion, it seems to be present some NW-SE and N-S anomalies (B, D, G, and N in Figure 5b). Their orientations are highlighted with continuous lines in Figure 5b. Their elongated nature could indicate a major fracture system or groups of fractures. The southeastern portion is featured by very small and isolated anomalies.

**Figure 5.** (a) Tilt angle contoured each 2%. Values in the scale at the left side are in %. The letters indicate most conspicuous anomalous features. (b) Fraser filtering applied to tilt angle. Contours are given each 5%. Values in the scale at the left side are in %. The letters indicate most conspicuous anomalous features. Yellow continuous lines are structure alignments inferred.



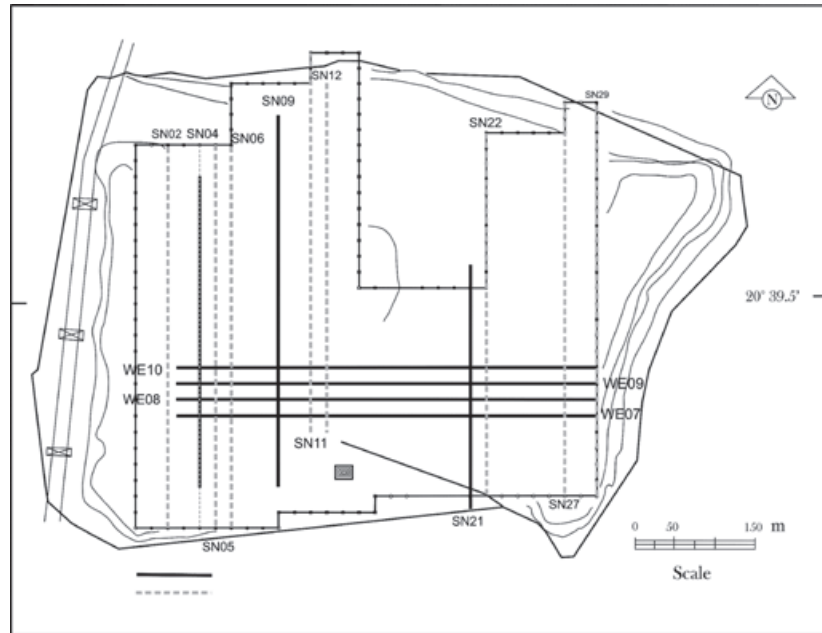
### Quantitative Interpretation

In a first quantitative step we applied the Fraser and Karous-Hjelt's technique modified to model VLF data by means of cell-shaped sources with constant resistivities (Edsen and Nissen, 1997). Several N-S and E-W profiles, corresponding to 24 KHz, were selected (Figure 6) for this purpose (Alatorre-Zamora, 2003) considering the behavior of real and imaginary components, and taking into account noise areas covered within the survey, and results obtained by other geophysical methods (Alatorre-Zamora *et al.*, submitted); just three

of the most representative modeled profiles are presented.

The modeling was based on the VLFMOD program from Edsen and Nissen (1997), which models VLF-EM or VLF-R data and generates a simple model considering the source frequency and just one resistivity for the host media. This simple model can then be modified or other bodies can be added. In this case the respective model was formed based upon information given by resistive tomography (Alatorre-Zamora, 2003) and potential field models (Alatorre-Zamora *et al.*, submitted).

**Figure 6.** Location of interpreted profiles at Matatlan dumpsite. Solid black lines are profiles interpreted with VLFMOD program, whereas gray dashed lines are profiles interpreted with KHFFILT program. Symbols like WE10 or SN11 are the names of the consecutive profiles.



In this first stage our models comprise cells simulating fault or fracture zones, approach part of the landfill, and the top of the andesitic basement. In all cases, we assume a variable resistivity for the host layer along the dumpsite due to the presence of soil plus urban waste composition for the overall site, and andesitic blocks mainly at the SW sector. Indeed, andesitic blocks could occur beneath the entire study area, but they are covered by terrigenous material and the proper waste disposal, and this fact is considered in the modeling. The resistivity for the host layer varies from 170 to 440  $\Omega$ -m. To the andesitic basement were assigned resistivities from 92 to 268  $\Omega$ -m along the profiles, whereas fault and fracture zones were assigned lower resistivities. Interpreted profiles are showed in Figures 7a to 7c.

Although adjustment errors between computed and observed component anomalies are large, the outlined behavior of the computed anomalies is fairly similar to observed ones. These misfits show the difficulty to model VLF data, specially the imaginary (or out-of-phase) component.

EW-8, EW-9 and EW-10 profiles show continuity both in anomaly behavior and in location and resistivities of modeled bodies (Figures 7a to 7c). An example is represented by the fault zone inferred at about 300 m, with a proposed resistivity from 70 to 36 W-m (black filled boxes in profiles EW-08 to EW-10; in general, small boxes in these three profiles).

This fault zone seems to have reached a depth between 10 to 20 m, and in general show a southern dip. The same structure is observable in the Fraser filtered map (A and F elongated features in Figure 5b).

Another important feature of the models constitutes the use of a resistivity value for the host material of the sources, consistent with the andesitic basement of the landfill. This establishes that the lowest body cells seem to show the topography of the andesitic basement, i.e., this basement has depths from 5 to 7.5 m.

The low resistivity values assigned to the structures inferred as faults let to assume that these structures allow the migration of leachate to lower levels in the basement, although the fault zones inferred are deeper than the top of the andesitic basement (i.e., they cut it). The resistivities decrease with leachate, and this seems to cause these anomalies.

Fault zones actually agree with those inferred by mean of resistive tomography and magnetics and gravity interpretation (Alatorre-Zamora, 2003; Alatorre-Zamora *et al.*, submitted).

In a second step we conduit a profile interpretation using the Pirttijärvi's (2004) KHFFILT non-commercial program. This applies the Karous-Hjelt filtering technique and provides the vertical distribution of apparent current densities (López-Sánchez,

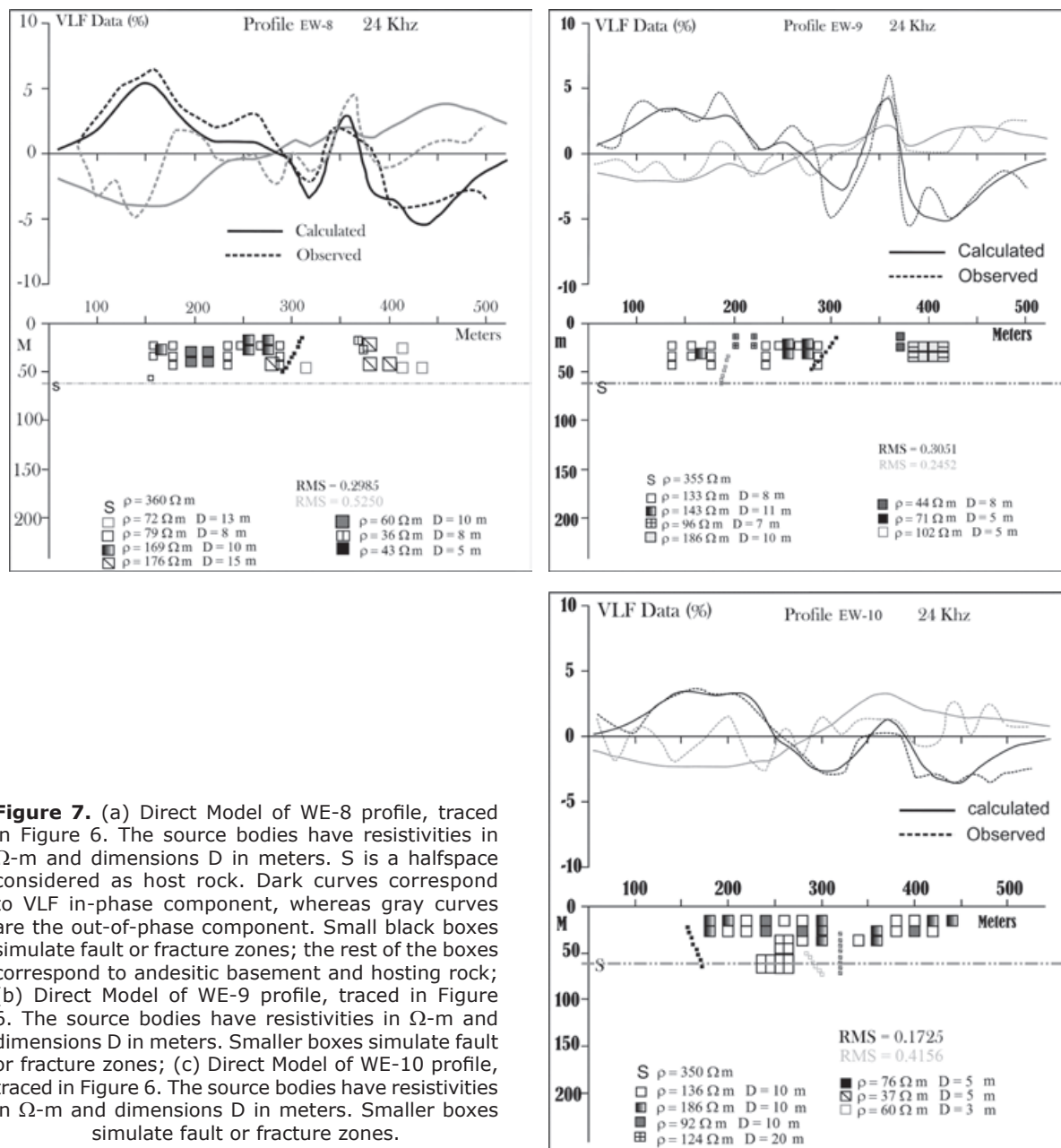


**Figure 7.** (a) Direct Model of WE-8 profile, traced in Figure 6. The source bodies have resistivities in  $\Omega\text{-m}$  and dimensions D in meters. S is a halfspace considered as host rock. Dark curves correspond to VLF in-phase component, whereas gray curves are the out-of-phase component. Small black boxes simulate fault or fracture zones; the rest of the boxes correspond to andesitic basement and hosting rock; (b) Direct Model of WE-9 profile, traced in Figure 6. The source bodies have resistivities in  $\Omega\text{-m}$  and dimensions D in meters. Smaller boxes simulate fault or fracture zones; (c) Direct Model of WE-10 profile, traced in Figure 6. The source bodies have resistivities in  $\Omega\text{-m}$  and dimensions D in meters. Smaller boxes simulate fault or fracture zones.

1998), which can be interpreted as to represent conductive zones below the surface (Benson *et al.*, 1997; Marroquin, 2000). In addition, the software provides a Fraser filtered profile, which correlates with the Karous-Hjelt filtered profile.

For each profile three plots are shown (see Figure 8a). The upper panel presents the raw data. The middle one presents the Fraser filtered profile. Finally, the lower panel corresponds to Karous-Hjelt (K-H) filtered profile, where we can note that low current density values correlates with high resistivity values

(Karous and Hjelt, 1977). Besides, peaks in the Fraser filter profile locate conductive structures.

Good correlation between the peaks of Fraser filter and conductive zones (survey as inferred by high current density values) of Karous-Hjelt filter is observed for profile NS-04 (Figure 8b). The profile NS-02 does not show conductive surfaces below the peaks of Fraser filtering (Figure 8a). This could be significant, because this last profile corresponds almost entirely to the western sector of the dumpsite (Figure 6),



whereas many conductive sources, as most recent deposition of waste and terrigenous material at the time, as well as the presence of heavy machinery, occurred at the NE part of the site.

Correlation of parallel Karous-Hjelt filtering profiles makes it possible to observe the continuity of features attributable to planar sources as fault and major fracture zones. In this manner we can appreciate the presence of 2D structures that are orthogonal to the VLF station used, it is to say, they are normal to NAA station, which has an NE-SW orientation with respect to Matatlan dumpsite. This indicates that we must infer mainly structures with NW-SE directions. According to the statistical analysis of fractures, we expect to locate fractures similar to groups C and D (see Figure 6).

To enable a better visualization of positive KH features, image maps with the resulting current densities from the modeled profiles were elaborated. These maps are showed in Figures 9a and 9b, and represent pseudodistributions of current density at depths of 20 and 40 m.

In these results it is possible to consider that there is not effect from conductive cover. Three main high current density features which have continuity in depth are: 1) an almost NE-SW elongated feature at the centre of the area (A in Figures 9a and 9b); 2) two elongated lineaments located in the western half of the site, that are parallel, with a N-S direction to the north, and become NW-SE to the south (E and H in Figures 9a and 9b). These last features reach depths of 40 m (Figure 9b), where they are clear; 3) a minor feature at the NW sector, whose direction is NW-SE (I in Figures 9a and 9b).

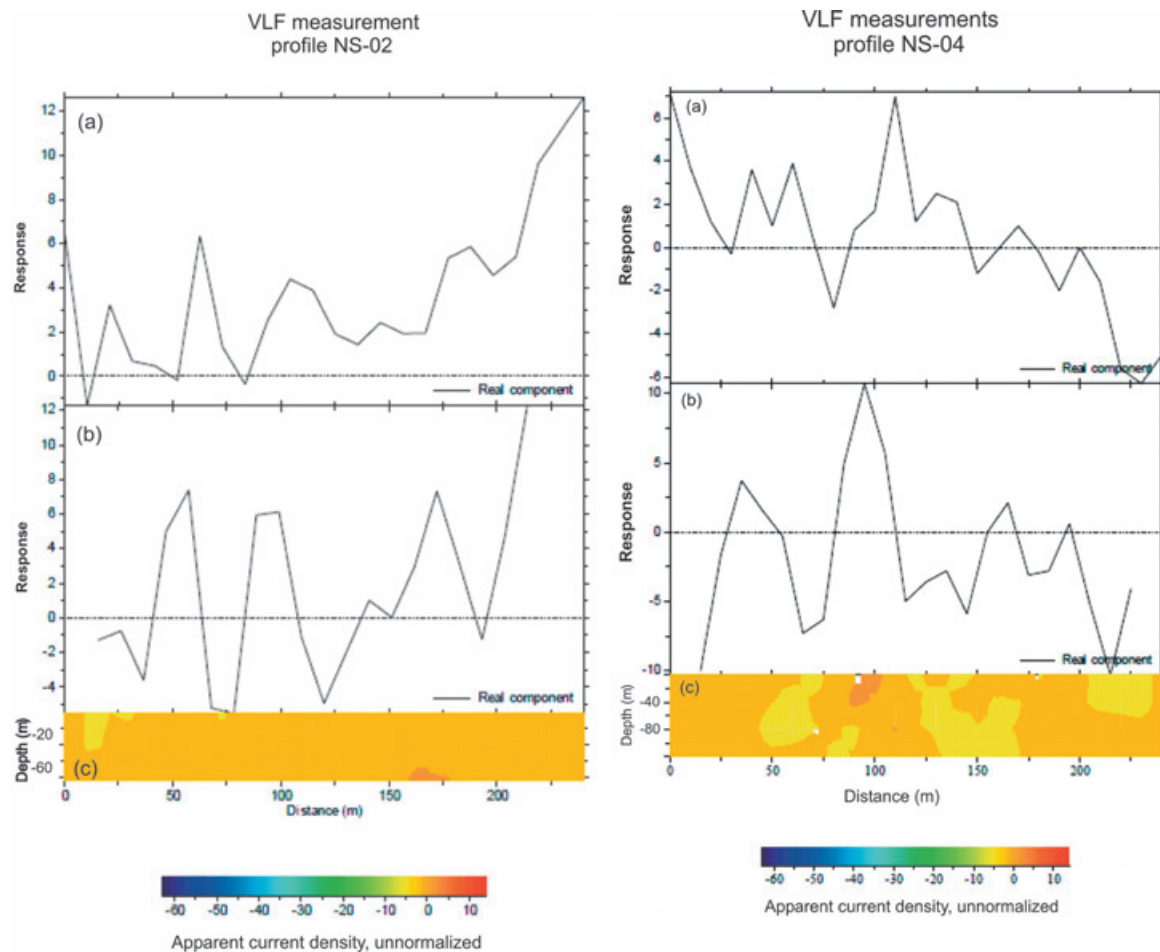


**Figure 8.** Fraser and Karous-Hjelt filtering results for the NS-02 (left plot) and NS-04 (right plot) profiles at Matatlan dumpsite. (a) raw data, given in %; (b) Fraser filter result, and (c) pseudosection of current density resulting to apply Karous-Hjelt filter.



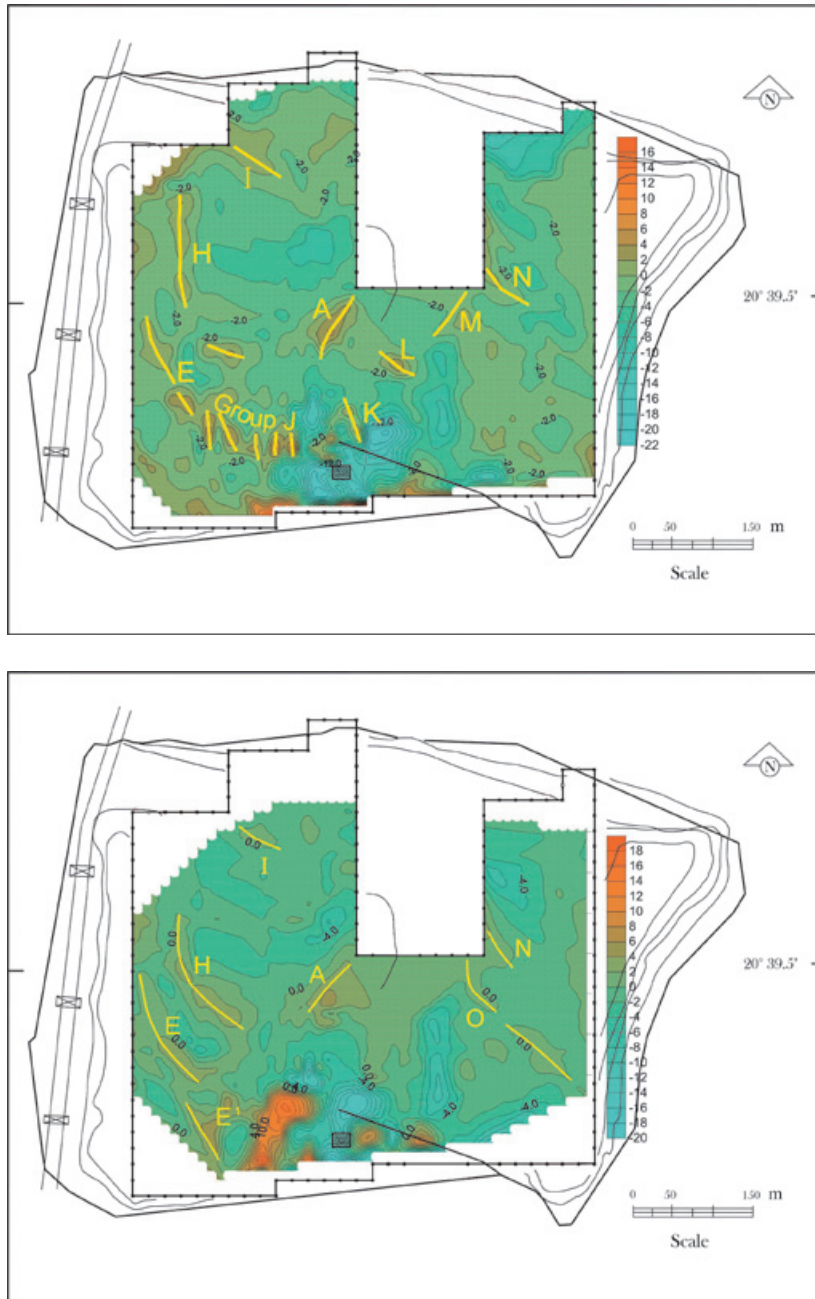


**Figure 9.** (a) Current density pseudodistributions located at 20 m in depth obtained with Karous-Hjelt filter; (b) Current density pseudodistributions located at 40 m in depth obtained with Karous-Hjelt filter.

These elongated high current density features could be owed to a major fracture system. A higher current density elongated feature that is not referred to in Figure 9b is observed also at 40 m in depth, in the SW edge of the site. It could be caused by the metallic fence that surrounds the pre-Columbian mound, but it does not appear at 20 m. Its almost N-S direction and its position (location) coincides with the outcropping there located.

Comparing maps from Figures 9a and 9b, a major high current density between 0 and 20 m is observed (Figure 9a); at this depth range, the higher value is located conspicuously, near the pre-Columbian mound, at the south side of the site.

Whereas some anomalies could be produced by leachate filtration or leachate presence into the dumpsite layer, the southern one near to the mound would be due to a wide fault zone.

Comparison between VLFMOD and KHFFILT results is possible, although in the first case we have a direct modeling, whereas the second one provides vertical current density pseudodistributions. KHFFILT seems to give better approximations when their results are combined together with Fraser results. Nevertheless, the modeled cells in the direct approach have parameters as resistivity and location that show fair correlation with Karous-Hjelt filtering results, showing that there is a good agreement (correlation) between the results of both methods used.

Comparison between 3D Fraser filtered results and KHFFILT results (Figures 5b, with Figures 9a and 9b) indicates very interesting correlations. Both techniques highlight same features that could be the signature of faults or major fracture systems. The major similarity occurs between results from Figure 5b and Figure 9b, showing a strong continuity for the VLF anomalies with depth.

We finally observe two generalized features: (1) several positive features with orientations mainly NW-SE that appears along the dumpsite, would show a possible influence of Tepic-Zacoalco rift. (2) The long N-S positive feature given by the two techniques and the 3D Fraser filtered tilt angle, at the westernmost sector of the dumpsite, could be result of the tectonic that controls the Rio Grande de Santiago Canyon. This last could be of listric nature.

## Conclusions

Very low frequency geophysical method has been proved to be an excellent media to infer 2D structures as faults and fractures through which water or contaminants flow might take place. Thereby providing a means to recognize and delineate the presence of 2D structures as faults and fractures that could function as migration paths for the leachates in urban waste dumpsites. Here we can conclude about the use of three techniques to interpret VLF data, that is, the Fraser filter applied to tilt VLF parameter, Karous-Hjelt filter applied to in-phase and out-of-phase VLF components, and a modified K-H filtering technique applied to the same components as a direct modeling, in the scope of the task described previously.

The statistic analysis of fracture direction measurements showed the presence of primary and secondary fracture groups. The primary groups have N-S, NE-SW, and NW-SE directions, in order of predominance.

Conspicuous anomalies in both, the in-phase component and the out-of-phase component occur with N-S orientation at the central and westernmost parts of the dumpsite. Areas of deposition and new mixed garbage at the date of the VLF survey are clearly visible as closed negative anomalies in the in-phase component. Tilt angle parameter showed the same behavior as the in-phase component.

The Fraser filtered results presents nine features of interest to the scope of the study. Four of them are NW-SE oriented, whereas three have NE-SW directions. The most conspicuous anomalous feature, however, has a long N-S direction, and is located at the westernmost part of the site.

With respect to the K-H filtering results, three main high current density features are inferred which have continuity with depth: 1) an almost NE-SW elongated feature at the centre of the area, 2) two elongated N-S parallel lineaments located in the western half of the site, that become NW-SE to the south. These last features continue in depth, being most clear at 40 m depth, 3) a minor feature at the NW sector, whose direction is NW-SE. These elongated high current density features could be owed to fracture systems. A higher current density elongated feature is observed also at a depth of 40 m, in the SW edge of the site. It could be caused by the metallic fence that surrounds the pre-Columbian mound, but it does not appears at 20 m. Its almost N-S direction and its location coincide with the andesitic outcrop there located.

The comparison between Fraser and Karous-Hjelt filters and two different techniques that provides model sources and current distribution respectively, showed good-to-fair results in the location of some fracture or fault zones.

Finally, it is interesting to note the correlation between the lineaments inferred by means of the cooperative use of both techniques, based on K-H and the Fraser filter and the major tectonic features. Accordingly, a N-S structure in the westernmost part of the zone, that have same direction as Rio Grande de Santiago Canyon, as well as NW-SE features, mainly in the western half of the site. These NW-SE features coincide with the directions of the Tepic-Zacoalco rift. Others NE-SW features appear towards the centre of the area. These facts correlate with the predominance of fracture groups showed in the fracture analysis.

Finally, the structures inferred and their directions could act to migrate lixivates outside the dump, mainly towards the Coyula Canyon, located along the south border of the site, as well as in a minor effect towards the Rio Grande de Santiago Canyon.

### Acknowledgements

The first author was supported with a grant from SUPERA-PROMEP and is indebted to CAABSA-EAGLE for allowing the study. The text improved thanks to criticism of Dr. Shevvin and an anonymous reviewer.

### References

- Alatorre-Zamora M.A., Campos-Enrriquez J.O., 1991, La Primavera Caldera (Mexico): structure inferred from gravity and hydrogeological considerations. *Geophysics*, 56, 992-1,002.
- Alatorre-Zamora M.A., 2003, Estudio Geofísico Integrado Realizado en el Vertedero de Desechos Urbanos de la Ciudad de Guadalajara. Ph D Thesis. Instituto de Geofísica, UNAM. 132-154 pp.
- Alatorre-Zamora M.A., Campos-Enrriquez J.O., Chávez-Segura R., Belmonte-Jiménez S.I., in press. Mapping major fractures affecting the basement of an urban waste dump (Matatlan, western Mexico). Assessment of use of Euler deconvolution, analytical signal, and the micromagnetic method. Submitted to *Near Surface Geophysics*.
- Alexandros S. Savvaidis, Tsokas G.N., Vargemezis G., Dimopoulos G., 1999, Geophysical prospecting in the Akropotamos dam (N. Greece) by GPR and VLF methods. *Journal of the Balkan Geophysical Society*, 2, 120-127.
- Armadillo E., Massa F., Caneva G., Gambetta M., Bozzo E., 1998, Modelling of Karst structures by geophysical methods. An example: the doline of S. Pietro dei Monti (Western Liguria). *Annali di Geofisica*, 41, 3 páginas.
- Baker H.A., Myers J.O., 1979, VLF-EM model studies and some simple quantitative applications to field results. *Geoexploration*, 17, 55-63.
- Bayrak M., 2002, Exploration of chrome ore in Southwestern Turkey by VLF-EM. *Journal of the Balkan Geophysical Society*, 5, 35-46.
- Beamish D., 1994, Two-dimensional, regularised inversion of VLF data. *Journal of Applied Geophysics*, 32, 357-374.
- Beamish D., 1998, Three-dimensional modeling of VLF data. *Journal of Applied Geophysics*, 39, 63-76.
- Bekaert C., Budka A., Lambomez-Michel L., Matichard Y., Martin I., 2002, Los vertederos y el desarrollo sostenible. *Revista Residuos*, 64 páginas.
- Benson A.K., Payne K.L., Stubben M.A., 1997, Mapping groundwater contamination using dc resistivity and VLF geophysical methods— A case study. *Geophysics*, 62, 80-60.
- Bozzo E., Lombardo S., Merlanti F., 1994, VLF prospecting: observations about field experiments. *Annali di Geofisica*, 37, 5 páginas.
- Campos-Enrriquez J.O., Alatorre-Zamora M.A., 1998, Shallow crustal structure of the junction of the grabens of Chapala, Tepic-Zacoalco and Colima, Mexico. *Geofísica Internacional*, 37, 263-282.
- Christensen T.H., Cossu R., Diaz L., Lechner P., Stegmann R., Lagerkvist A., 2000, Alternative approach to the elimination of greenhouse gases from old landfill. Curso superior sobre gestión y diseño de vertederos. CER (Club Español de los Residuos).
- Edsen N.A., Nissen J., 1997, VLFMOD, a free forward VLF modeling software package. ftp: <http://home1.swipnet.se/~w-11019/ABEM-ftp/>
- Ferrari L., 1995, Miocene shearing along the northern boundary of the Jalisco block and the opening of the southern Gulf of California. *Geology*, 23, 751-754.
- Fraser D.C., 1969, Contouring of VLF-EM data. *Geophysics*, 34, 958-967.
- Gilbert C.M., Mahood G.A., Carmichael I.S.E., 1985, Volcanic stratigraphy of the Guadalajara area, Mexico. *Geofísica Internacional*, 24, 169-191.
- Greenhouse J.P., Harris R.D., 1983, Migration of contaminants in groundwater at a landfill: a case study, 7. DC, VLF, and inductive resistivity surveys. In: J.A. CHERRY (Guest Editor), Migration of contaminants in

- groundwater at a landfill: A Case Study. *Journal of Hydrology*, 63, 177-197.
- Hjelt S.E., Kaikkonen P., Pietila R., 1984/85, On the Interpretation of VLF Resistivity Measurements, *Geoexploration*, 23, 171-181.
- Jones D.R.V., Dixon N., 2005, Landfill lining stability and integrity: the role of waste settlement. *Geotextiles and Geomembranes*, 23, 27-53.
- Kaikkonen P., 1979, Numerical VLF modeling, 1979, *Geophysical Prospecting*, 17, 815-834.
- Kaikkonen P., Sharma S.P., 1998, 2-D nonlinear joint inversion of VLF and VLF-R data using simulated annealing, *Journal of Applied Geophysics*, 39, 155-176.
- Karous M., Hjelt S.E., 1983, Linear filtering of VLF dip-angle measurements, *Geoph. Prospecting*, 31, 782-794.
- Kjeldsen P., Barlaz M.A., Rooker A.P., Baun A., Ledin A., Christensen T.H., 2002, Present and long-term composition of MSW landfill leachate. A review. *Critical Reviews In Environmental Science and Technology*, 32, 297-336.
- Lopez-Sanchez M., 1998, [www.geophysicsgpr.com/aben/wadi\\_vlf.htm](http://www.geophysicsgpr.com/aben/wadi_vlf.htm).
- Luhr J., Lazaar P., 1985, The southern Guadalupe volcanic chain, Jalisco, Mexico. *Geofísica Internacional*, 24, 691-700.
- Mahood G.A., 1980b, Geological evolution of a Pleistocene rhyolitic center - Sierra La Primavera, Jalisco, Mexico. *Journal of Volcanologic and Geothermal Research*, 8, 199-230.
- Marroquin I.D., 2000, Proyecto de Maestría. [www.wlba.net/ivan/vprm.es.html](http://www.wlba.net/ivan/vprm.es.html).
- Milsom J., 2003, *Field Geophysics*, 3<sup>o</sup> edition; John Wiley & Sons, 244 Pp.
- Olsson O., 1980, VLF Anomalies from a perfectly conducting half plane below an overburden. *Geophysical prospecting*, 18, 415-434.
- Paál G., 1968, Very low frequency measurements in northern Sweden. *Geoexploration*, 6, 141-149.
- Paterson N.R., Ronka V., 1971, Five years of surveying with the Very Low Frequency Electromagnetics Method. *Geoexploration*, 9, 7-26.
- Phillips W.J., Richards W.E., 1975, A study of the effectiveness of the VLF method for the location of narrow-mineralized fault zones. *Geoexploration*, 13, 215-226.
- Pirttijärvi M., 2004, Karous-Hjelt and Fraser filtering of VLF measurements, version 1.1a, <http://www.cc.oulu.fi/~mpi/Softat/Khffilt.html>
- Reynolds J.M., 1998, *An Introduction to Applied and Environmental Geophysics*, John Wiley & Sons, eds., 796 pp.
- Rosas-Elguera J., Urrutia-Fucugauchi J., 1998, Tectonic control of the volcanosedimentary sequence of the Chapala graben, western Mexico. *Intern. Geol. Rev.*, 40, 350-362.
- Saydam A.S., 1981, Very low frequency electromagnetic interpretation using tilt angle and ellipticity measurements. *Geophysics*, 46, 1594-1605.
- Sinha A.K., 1990a, Interpretation of ground VLF EM data in terms of inclined sheet like conductor models. *PAGEOPH*, 132, 213-231.
- Vozoff K., 1971, The effects of overburden on vertical component anomalies in AFMAG and VLF exploration: a computer model study. *Geophysics*, 36, 53-57.
- Ward S.H., Ryu J., Glenn W.E., Homann G.W., Dey A., Smith B.D., 1974, Electromagnetic methods in conductive terrains. *Geoexploration*, 12, 121-183.
- Watkins N.D., Gunn B.M., Baksi A.K., Ade-Hall J., 1971, Paleomagnetism, geochemistry, and potassium-argon ages of the Río Grande de Santiago volcanics, central Mexico. *Geological Society of America Bulletin*, 82, 1,955-1,968.
- Wright J.L., 1988, *VLF interpretation manual: EDA Instruments (now Scintrex)*, Toronto.